Catena 123 (2014) 11–22

Contents lists available at ScienceDirect

Catena

journal homepage: www.elsevier.com/locate/catena

The dynamics of desertification in the farming-pastoral region of North China over the past 10 years and their relationship to climate change and human activity

Duanyang Xu [a,*], Chunlei Li [b], Xiao Song [c], Hongyan Ren [d]

[a] Institute of Science and Technical Information of China, Beijing 100038, PR China
[b] Research Institute of Forest Ecology Environment and Protection, Chinese Academy of Forest, Beijing 100091, PR China
[c] Henan Agricultural University, Zhengzhou 450002, PR China
[d] Institute of Geographic Sciences and National Resources Research, Chinese Academy of Science, Beijing 100101, PR China

ARTICLE INFO

Article history:
Received 10 February 2013
Received in revised form 10 June 2014
Accepted 11 July 2014
Available online 26 July 2014

Keywords:
Desertification
Climate change
Human activity
Farming-pastoral region
NPP

ABSTRACT

The farming-pastoral region of North China is a region that has suffered from serious desertification, and the multiple transitional characteristics in this region make it very difficult to link the progress of desertification to the driving forces behind it. This paper mainly focuses on the dynamics of desertification over the past 10 years and their relationship to climate change and human activity. According to the MODIS images in 2000 and 2010, the farming-pastoral region had experienced significant desertification dynamics over the past 10 years. The area of regions that had undergone desertification reversion and expansion were 186,240 km^2 and 199,525 km^2 respectively, and the spatial distribution of these regions showed great heterogeneity. The relationship between desertification dynamics and their driving forces was investigated by comparing the change in the NPP that was induced by climate change and human activity for each pixel that experienced desertification reversion and expansion. From 2000 to 2010, the coupling of climate change and human activity was the dominant factor behind desertification reversion. However, the human activity was the dominant factor that controlled the desertification expansion process between 2000 and 2010. The driving processes of desertification also had considerable spatial heterogeneity, and the dominant factors behind desertification reversion and expansion in each sub-region were not completely the same. So, the scale effect must be considered when explaining the results from similar studies.

1. Introduction

The farming-pastoral region of North China is an ecologically fragile region. The dry climate conditions and long-term excessive human activity induced by rapid population increase, such as overgrazing, over cultivation and overcutting, have made desertification in this region a serious environmental problem that affects the regional and national economy and society development (Jiang et al., 2005; Liu et al., 2011; Qi et al., 2012; Tang and Zhang, 2003; Wang et al., 2005). According to desertification monitoring conducted by Chinese researchers, the area of desertified land in the farming-pastoral region can reach up to 60% of the total area of desertified land in China (Wang, 2004; Wang et al., 2004a, 2004b). The interaction of different driving forces make the desertified land change greatly between different classes of desertification state in this region (it is defined as desertification dynamics in this study), which might have a significant impact on the desertification pattern and progress at national scale, including the carbon and nitrogen biogeochemical cycles in the arid and sub-arid regions (Peters and Havstad, 2006; Sivakumar, 2007; Su et al., 2007). Although the dynamics of desertification can be accurately monitored by using remote sensing images at different scales, it is still very difficult to link the dynamics of desertification to their driving forces owing to a lack of reliable and spatially explicit methods that can distinguish the impacts of climate change and human activity on desertification (Geerken and Ilaiwi, 2004; Prince, 2002). So, it is very difficult to explore the potential mechanisms of desertification and launch countermeasures for rehabilitation.

The vegetation condition of the degraded land have always been treated as a good indicator that can be used to quantitatively detect ecosystem processes at different scales (Asner and Heidebrecht, 2005; Hanafi and Jauffret, 2008; Prince, 2002; Veron et al., 2006). So, many studies have tried to use vegetation indices retrieved from remote sensing images, especially the Normalized Difference Vegetation Index (NDVI) and Net Primary Production (NPP, which has a strong correlation with NDVI), to distinguish anthropogenic land degradation or desertification by comparing the potential and actual status of vegetation (Evans and Geerken, 2004; Geerken and Ilaiwi, 2004; Herrmann et al., 2005; Holm et al., 2003; Wessels et al., 2004, 2007; Xu et al., 2009, 2010). Rain Use Efficiency (RUE) is defined as the ratio of NPP or NDVI to rainfall, which has been proved to be a robust indicator that can

* Corresponding author. Tel.: +86 10 58882012; fax: +86 10 58882072.
E-mail address: xudy@istic.ac.cn (D. Xu).

http://dx.doi.org/10.1016/j.catena.2014.07.004
0341-8162/

reflect the desertification process and its potential driving mechanisms. For example, deviations from the potential value of RUE can be treated as a useful index to identify man-made degradation (Holm et al., 2003; Nicholson et al., 1998; Prince et al., 1998, 2007); and the combination of RUE (both in full and extreme periods) with aridity index could be employed to identify the land degradation dynamics and detrend the impact from climate (Del Barrio et al., 2010; Hill et al., 2010). The RESTREND (Residual Trends) method is another helpful tool that can effectively identify human-induced land degradation, and negative trends in residual values (the difference between the observed NDVI and the NDVI predicted by rainfall using regressions calculated for each pixel) can be regarded as a sign of human-induced degradation (Wessels et al., 2004, 2007). Although these methods can identify the human-induced degradation at pixel scale using remote sensing technology, they still cannot be used to assess the relationship between desertification dynamics and their driving forces because the effects of climate change are ignored in the analysis process. In addition, some problems or controversies in these methods may limit their further application. For example, recent study has shown that RUE varied between years as a function of both ecosystem degradation and annual rainfall variation; and it may lead to a bias estimation for the causes of desertification by assuming that RUE was a constant value in the absence of degradation (Hein and de Ridder, 2006). The LNS (Local NPP Scaling) method that was proposed by Prince (2002) had overcome the problem induced by the unstable estimation for potential status of vegetation; the potential NPP used in LNS method was calculated as the 90th percentile of the frequency distribution of ΣNDVI for each land capability classification (Prince et al., 2009; Wessels et al., 2008). However, this method cannot distinguish the impacts of climate change and human activity in a specific period.

Based on the merits of the methods mentioned above, especially the idea for identifying human-induced land degradation, a new method was developed by Xu et al. (2009, 2010) that can be used to assess the relationship between desertification dynamics and their driving forces. In this method, the regions that have experienced desertification reversion and expansion during a fixed period are firstly identified, and then the potential NPP and the difference between potential and actual NPP are selected as the indicators to assess the relative role of climate change and human activity under different desertification driving scenarios. All these calculations are based on grid data, which make it possible to link the desertification dynamics to their driving forces in space. However, this method has only been applied and proved to be feasible at the city scale and it needs to be checked further at a larger scale.

The farming-pastoral region of North China has experienced obvious desertification dynamics according to the satellite remote sensing records; especially over the past 10 years, rapid urbanization, large-scale exploitation of resources and the various ecological protection measures have increased the spatial heterogeneity of the desertification dynamics and their driving mechanisms in this region. However, few studies have assessed the dynamics of desertification in the farming-pastoral region of North China over the past 10 years and analyzed their driving mechanisms by linking the processes to climate change and human activity. Using the method of assessing the relative role of climate change and human activity in desertification developed by Xu et al. (2009, 2010), the objectives of this study were: (1) to monitor the dynamics of desertification in the farming-pastoral region of North China between 2000 and 2010 by retrieving the MODIS images and (2) to analyze their relationship to climate change and human activity in space.

2. Materials and methods

2.1. Study area

The farming-pastoral region of North China is located in the southeastern Inner Mongolia Plateau and northwest of the Loess Plateau of China, and ranges from 36°05′ to 50°15′ N and 106°10′ to 124°05′ E (Fig. 1). The farming-pastoral region of North China is a typical ecological transition zone that shows multiple transitional characteristics in agricultural production and climate conditions, which have made the ecological environment more fragile (Chen et al., 2008; Liu et al., 2011; Tang and Zhang, 2003). The annual precipitation in the farming-pastoral region of North China is between 200 and 400 mm. Nearly 60–70% of the rainfall occurs between June and August and the precipitation in this region has always had a high inter-annual fluctuation. The temperature in the farming-pastoral region of North China ranges from 0 to10 °C; and the altitude of the region is generally >1000 m. The aridity of the farming-pastoral region of North China gradually increases from east to west, which gives the vegetation and soil in this region significant zonal characteristics.

Agriculture and animal husbandry are the two main modes of production for the local rural residents in the farming-pastoral region of North China. Population pressure, especially the growth of the rural population over a long period has damaged the vegetation and the soil has become exposed due to extensive reclamation and grazing. Furthermore, urban expansion and the development of the mining industry in the region over recent years have made the land surface more fragile (Hao and Ren, 2009). These factors, together with bad climate conditions, especially wind erosion, made the desertification develop rapidly during the past few decades and have become a serious environmental problem for the local and national government. Based on the characteristics of the farming-pastoral region of North China mentioned in previous studies and the distribution of desertified land in this region (Wang, 2004; Wang et al., 2005), this study defined the boundary of the research region according to the division of administrative regions, which included 21 cities and 89 counties (banners) in Liaoning, Inner Mongolia, Hebei, Shanxi, Shannxi, Ningxia and Gansu provinces.

2.2. Data collection and pre-processing

In this study, MODIS 16-day composited NDVI (MOD13A1), land surface albedo (MCD43A3) and reflectance of band 7 (MCD43A4) with a resolution of 500 m × 500 m were selected as three key indicators to monitor the desertification dynamics from 2000 to 2010, which represented vegetation cover, land surface energy balance and soil water content (Ji et al., 2009; Zarco-Tejada et al., 2003), respectively. These data used for desertification monitoring were acquired at autumnal equinox in 2000 and 2010. This decision was mostly based on the consideration that the abundant vegetation information in the images at that time was suitable for desertification monitoring. In addition, 10 scenes band 7, 4, 2 composited Landsat ETM+ images acquired in 2000 from MDA Federal Inc. and 18 scenes Aster images acquired in 2010 were collected as auxiliary data to support the selection of referencing points for desertification monitoring and accuracy checking. Geometric correction of each Aster image was accomplished by selecting Landsat ETM+ images as referencing map, and the precision tolerance was less than 1 pixel.

For analyzing the relationship between desertification dynamics and driving forces, NPP is a key indicator. In this study, MODIS 16-day composited NDVI data in the same month were further composited by using Maximum Value Composites (MVC) method to produce the monthly NPP from 2000 to 2010. There were a total of 132 (12 month in 11 years) monthly NDVI and NPP data in the research period, and only yearly NPP (sum of all monthly NPP in a year) was used to analyze the relationship between desertification dynamics and driving forces. Besides, meteorology data, vegetation and soil information were also collected for NPP calculation. The monthly-averaged meteorological data for 2000–2010 recorded by 162 meteorological stations in and around the research region, such as precipitation, temperature, sunshine duration, and wind speed, were obtained from the China Central Meteorological Bureau. 1:1,000,000 vector vegetation map and soil map of China, and the related attributions for each unit in the maps

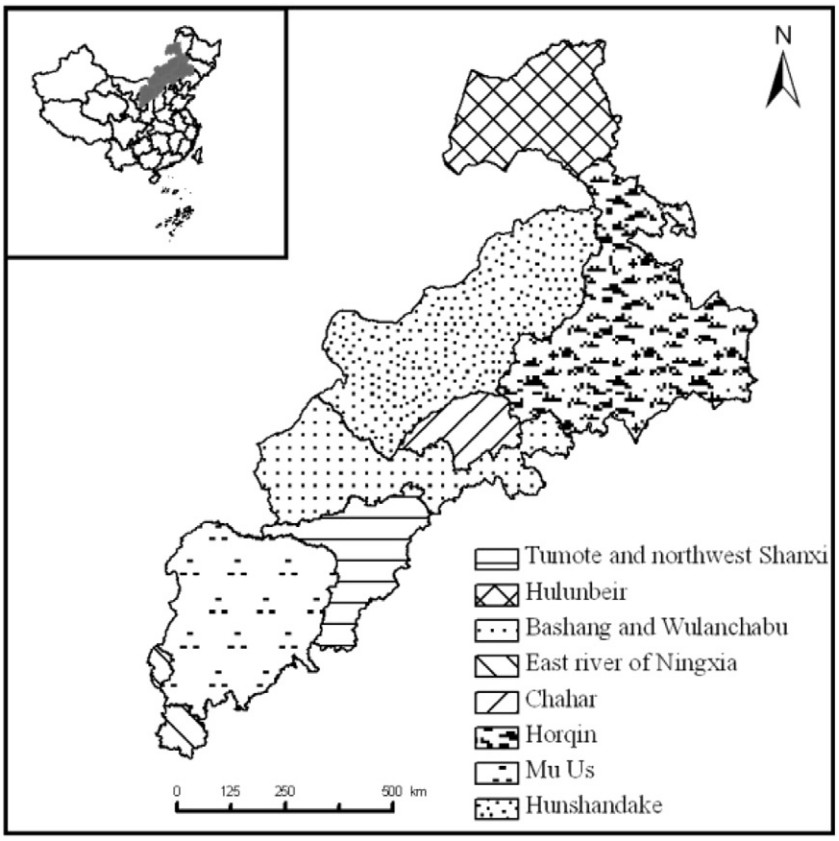

Fig. 1. The location of the farming-pastoral region of North China.

were obtained from the Data Center for Resources and Environmental Sciences Chinese Academy of Sciences, which were used to produce the vegetation and soil map for the farming-pastoral region of North China by clipping the whole maps with the research region boundary.

In order to statistically analyze the data, all the data used in this study were resampled or converted into grid data with 1 km × 1 km resolution. For the meteorological data, Inverse Distance Weighted (IDW) method was employed to produce grid data; and for the vector data, such as vegetation max light use efficiency derived from vegetation map, Maximum Area method was used to set the new value of grid data. In this study, the projected coordinate system of these data was all set to Clarke 1866 Albers.

2.3. Desertification dynamics monitoring

The desertification classification system used in the National Basic Program of China was adopted in this study, and the lands in the research region were classified into five grades: non-desertification, low desertification, medium desertification, high desertification and severe desertification (Wang, 2004; Wang et al., 2004a, 2004b). In this study, the Decision Tree (DT) model was employed to identify the grades of desertification by combing the indicators mentioned above. Considering the effects of land surface heterogeneity on desertification monitoring at large scale, research region was divided into eight sub-regions that had a homogeneous environment according to previous studies (Wang, 2004), they were the Hulunbeir sandy region, the Hunshandake sandy region, the Horqin sandy region, the Chahar sandy region, the Bashang and Wulanchabu sandy region, the Tumote and northwest Shanxi sandy region, the Mu Us sandy region and the East River of Ningxia sandy region (Fig. 1). Based on building the corresponding relationship between typical desertification regions and the characteristics of remote sensing images, 25 training points for each desertification grade in eight sub-regions were selected by referencing the field investigation and visual interpretation results of remote sensing images. These training points were used to extract the value of three indicators for every desertification grade in each sub-region, and then the primary rule sets for the DT model were constructed according to the frequency distribution statistics of these extracted indicator values of different desertification grades. After adjusting the indicators' threshold values of different desertification grades until it reached an acceptable accuracy, the final rule sets were acquired. In the process of field investigation, the characteristics of vegetation, soil, landscape and topography within 1 km × 1 km samples were used to judge desertification grade by referencing the classification criterion that was used in the National Basic Program of China.

2.4. Assessment of the relationship between desertification dynamics and climate change and human activity

NPP has been considered as a good common indicator for measuring the impacts of driving forces on desertification, which not only reflects the ecological process of desertification but also makes it possible to link the desertification dynamics to their driving forces in space (Prince, 2002; Xu et al., 2009). In this study, the potential NPP (CNPP) and the difference between the potential and actual NPP (HNPP) were used to assess the impacts of climate change and human activity on the NPP of desertified land respectively. The change in these values over a fixed period can be used to reflect their relative roles in desertification reversion and expansion. Based on the identified regions experiencing desertification reversion (the change of desertification state to a lighter class between 2000 and 2010) and expansion (the change of desertification state to a severer class between 2000 and 2010), the relationship between desertification dynamics and climate change and human activity at pixel level can be mapped by comparing the changing trends in CNPP and HNPP, which can be done by calculating the linear regression coefficient of the time series. These are referred

to as SlopeCNPP and SlopeHNPP, respectively. When SlopeCNPP is positive or SlopeHNPP is negative, it means that climate change or human activity benefit vegetation growth and desertification reversion; on the contrary, it means that climate change or human activity benefit vegetation degradation and desertification expansion.

$$HNPP = CNPP - NPP. \quad (1)$$

$$Slope = \frac{n\sum xy - \left(\sum x \sum y\right)}{n\sum x^2 - \left(\sum x\right)^2} \quad (2)$$

where:

n = 11
x = year (2000, 2001....., 2010)
y = CNPP or HNPP

For each grid that experienced desertification reversion:

If SlopeCNPP > 0 and SlopeHNPP < 0, then both climate change and human activity improved vegetation growth and dominated desertification reversion together.
If SlopeCNPP > 0 and SlopeHNPP > 0, then climate change was the dominant factor for vegetation growth and desertification reversion.
If SlopeCNPP < 0 and SlopeHNPP < 0, then human activity was the dominant factor for vegetation growth and desertification reversion.
If SlopeCNPP < 0 and SlopeHNPP > 0, then both climate change and human activity went against vegetation growth and desertification reversion. This result can be treated as the error in this method that might be induced by the accuracy of desertification monitoring.

For each grid that experienced desertification expansion:

If SlopeCNPP < 0 and SlopeHNPP > 0, then both climate change and human activity were adverse to vegetation growth and dominated desertification expansion together.
If SlopeCNPP < 0 and SlopeHNPP < 0, then climate change was the dominant factor for vegetation degradation and desertification expansion.
If SlopeCNPP > 0 and SlopeHNPP > 0, then human activity was the dominant factor for vegetation degradation and desertification expansion.
If SlopeCNPP > 0 and SlopeHNPP < 0, then although both of climate change and human activity improve benefit vegetation growth, the land still experienced desertification expansion. This result was also treated as the error with regard to referencing desertification reversion.

In this study, the actual NPP was calculated by using Carnegie–Ames–Stanford-Approach (CASA) model (Field et al., 1995; Lobell et al., 2003; Potter et al., 1993; Tao et al., 2005), and the model of potential NPP was designed in the same manner as CASA model except for the calculation of Fraction Photosynthetically Active Radiation (FPAR). For potential NPP calculation, FPAR was retrieved according to the meteorological parameters, maximum and minimum of Leaf Area Index. The detail for the actual and potential NPP calculation can be referenced from previous studies (Xu et al., 2009, 2010).

2.5. Validation

Validation of the results was necessary and had been taken in this study, which contained two parts: desertification dynamics monitoring and assessment of the relationship between desertification dynamics and climate change and human activity. For the validation of desertification dynamics monitoring, 5 checking points for each desertification grade in every sub-region were synchronously selected when choosing the training points, and desertification grades of these checking points were also judged at the same time. The overall accuracy (the ratio of correctly classified points to the total checking points) was used to validate the desertification monitoring results. For the validation of assessment of the relationship between desertification dynamics and driving forces, considering the difficulty of quantifying the assessment result and identification of the desertified regions induced by climate change, some typical human-induced desertified regions were selected by comparing the Landsat ETM + images in 2000 with Aster images in 2010 before the assessment; and then, the comparisons between these regions and assessment results were conducted to get a validation.

3. Results

3.1. Desertification dynamics in the farming-pastoral region of North China between 2000 and 2010

According to the results of accuracy checking for desertification monitoring in this study, the overall accuracy reached 85.5%. Although this accuracy might be lower than that using high-resolution satellite images, it can satisfy the need of researches at a large scale. From 2000 to 2010, the total areas of desertified land in the farming-pastoral region of North China did not change significantly (the area of desertified land in 2000 and 2010 was 536,597 km^2 and 540,560 km^2, respectively), but the desertified lands with different grades underwent an obvious change. According to the statistics, the area of medium desertification land increased and all of the other grades decreased between 2000 and 2010. The greatest decrease (27.8%) was in the land that was classified as 'high desertification'. A comparison of the change in the different desertification grades from 2000 to 2010 was conducted in this study, which showed that although some desertified lands had reversed between 2000 and 2010, the area of these reversed lands was almost the same as the lands that had experienced desertification expansion (186,240 km^2 and 199,525 km^2, respectively). The spatial distribution of these reversed and expanded desertification lands between 2000 and 2010 were very different, which is illustrated in Fig. 2 (the numbers 1, 2, …, 8 in Fig. 2 represents the Hulunbeir, Hunshandake, Horqin, Chahar, Bashang and Wulanchabu, Tumote and Northwest Shanxi, Mu Us and East River of Ningxia sandy regions, respectively). The Mu Us sandy region had experienced a significant desertification reversion between 2000 and 2010, especially the mid-west of this region. The other regions that had undergone significant desertification reversion were mainly distributed in the northwest of Shanxi province and in the south of the Horqin sandy region. The spatial distribution of lands that had experienced desertification expansion showed that they were mainly located in northeastern Mu Us, the middle of Hulunbeir and at the border between the Hunshandake and Horqin sandy regions.

3.2. NPP, CNPP, HNPP values for desertified land and their changing trends

The change in vegetation is one of the most important characteristics of the desertification process (Asner and Heidebrecht, 2005; Prince, 2002; Sivakumar, 2007). According to the average NPP value for the lands with different desertification grades in 2000, the increase in desertification grades led to an obvious decrease in NPP. For example, the NPP for low desertification land was 149.21 g C m^{-2} $year^{-1}$, but the values for highly and severely desertified land were only 66.26 and 47.01 g C m^{-2} $year^{-1}$, respectively. The average CNPP and HNPP values for areas with different desertification grades in 2000 are showed in Fig. 3. The CNPP values for the different desertification grades showed the same trend as NPP values, which could be mainly attributed to the differences in the vegetation types present in the different grades of

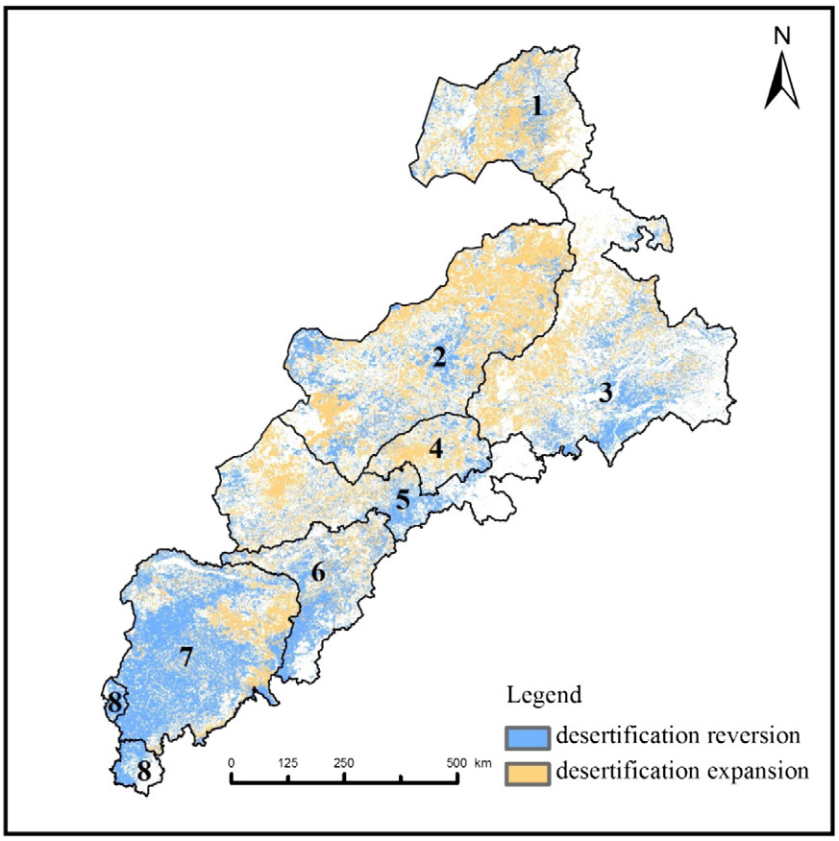

Fig. 2. The spatial distribution of the lands had experienced desertification reversion and expansion between 2000 and 2010 in the farming-pastoral region of North China.

desertified lands. The average HNPP values for desertified land were significantly higher than for non-desertification land and this reflects the relative degrees of impact by humans.

Over the past 10 years, the NPP, CNPP, HNPP values of the farming-pastoral region of North China had experienced a signification change and exhibited considerable spatial heterogeneity (Fig. 4). With regard to NPP, the northeast of Mu Us and the southeast of the Horqin sandy regions experienced a significant increase in NPP. However, the NPP values for most of Hulunbeir, the common boundary between Hunshandake and Horqin, the middle region of the Bashang and the Wulanchabu sandy regions showed significant declines. The CNPP trend can reflect the change in climate and its impacts on vegetation. From 2000 to 2010, the regions that showed a positive trend for CNPP were mainly distributed in North Mu Us, southeast Horqin and the middle of the Hunshandake sandy regions, which means that climate change might have benefited the vegetation growth in those regions. However, negative trends in CNPP were observed in east Hulunbeir, the common boundary between Hunshandake and Horqin, Tumote and northwest of Shanxi and south of the East River of Ningxia sandy regions. The spatial heterogeneity of the HNPP trend was higher than it was for the NPP and CNPP trends, which can be attributed to regional differences in human activity. As shown in Fig. 4c, some obvious positive trends in HNPP were found in northwest Horqin; and some obvious negative trends in HNPP were observed in the southeast of the whole farming-pastoral region of North China, which implied that ecology protected activity had occurred in these regions during the past 10 years.

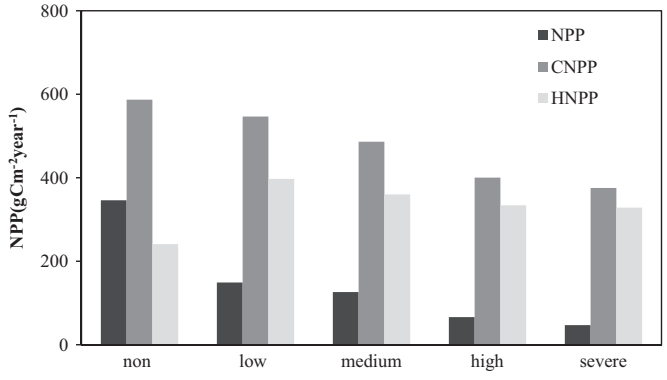

Fig. 3. The comparison of average NPP, CNPP and HNPP values for the areas with different desertification grades.

3.3. Desertification reversion and its relationship with climate change and human activity

Based on extracting the regions that experienced desertification reversion from2000 to2010, the relationship between desertification reversion and climate change and human activity were examined and mapped by comparing the changing trends of CNPP and HNPP. According to Table 1, the coupling of climate change and human activity was the relatively dominant factor controlling desertification reversion. The area of the regions that had experienced desertification reversion induced by climate change and human activity together amounted to 66,569 km^2. The contribution of climate change and human activity were almost the same with regard to desertification reversion in the farming-pastoral region of North China between 2000 and 2010. The areas that had experienced desertification reversion dominated by climate change or human activity were just 54,570 km^2 and 52,302 km^2, respectively.

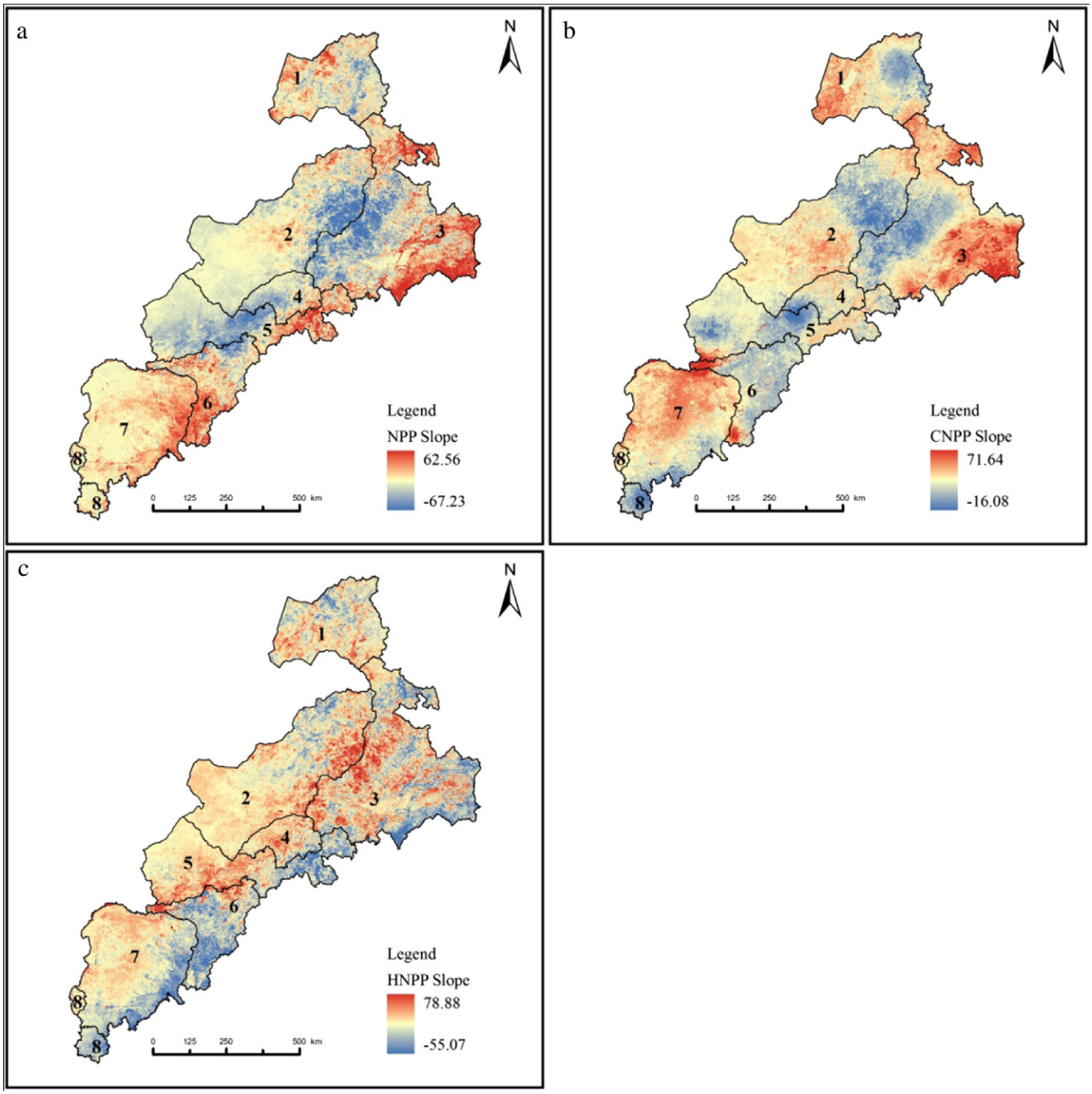

Fig. 4. The trends of NPP, CNPP and HNPP values of the farming-pastoral region of North China between 2000 and 2010.

Desertification reversion and its driving forces can be spatially linked in the space for each grid in this study, and it showed a great spatial heterogeneity with regard to different processes driving desertification reversion. As shown in Fig. 5, the regions that had experienced desertification reversion dominated by climate change were relatively concentrated and they were mainly distributed in the middle of the Mu Us sandy region. However, the regions that had experienced desertification reversion that mainly induced by human activity were relatively decentralized and mainly located in the southeastern part of Mu Us, most of Tumote and northwest of Shanxi and in the northeast of Hulunbeir and Horqin sandy regions. The desertification reversion regions that had been induced by climate change and human activity together were mainly distributed in the southwest of Mu Us and in the Horqin sandy regions.

3.4. Desertification expansion and its relationship with climate change and human activity

The relationship between desertification expansion from 2000 to 2010 and their driving forces are illustrated in Fig. 6. Human activity was the dominant factor controlling desertification expansion in the farming-pastoral region of North China between 2000 and 2010. The area of lands that had experienced desertification expansion due to only human activity was 62,723 km^2, which was higher than the expansion in desertified regions only dominated by climate change and those dominated by both climate change and human activity. However, in the subregions, the causes of desertification expansion were different. For example, climate change was the dominant factor that induced desertification expansion in the Tumote and northwest of Shanxi sandy region, but the

Table 1
The area of regions had experienced desertification reversion and expansion dominated by climate change and human activity (km^2).

	Desertification reversion				Desertification expansion			
	Reversion_C	Reversion_CH	Reversion_H	Error	Expansion_C	Expansion_CH	Expansion_H	Error
Hulunbeir	2908	4804	4291	2108	6948	4614	9259	9497
Hunshandake	9304	5871	4951	2560	19,014	17,737	27,640	9444
Horqin	8012	14,697	5219	1111	5479	14,554	9353	2670
Chahar	1186	1771	1696	478	1656	3752	4474	580
Bashang and Wulanchabu	3205	3438	6205	4641	4541	11,099	4919	516
Tumote and Northwest Shanxi	1458	5967	12,896	1478	4641	2122	1303	1180
Mu Us	27,934	28,116	12,868	137	5332	76	5773	11,120
East River of Ningxia	563	1905	4176	9	0	0	2	2
Total	54,570	66,569	52,302	12,522	47,611	53,954	62,723	35,009

Reversion/expansion_C was the desertification reversion/expansion dominated by climate change; reversion/expansion_CH was the desertification reversion/expansion dominated by climate change and human activity together; reversion/expansion_H was the desertification reversion/expansion dominated by human activity.

coupling of climate change and human activity dominated desertification expansion in the Horqin, Bashang and Wulanchabu sandy regions.

The spatial distribution of desertification expansion regions that were dominated by different driving processes also varied (Fig. 6). The regions that had experienced desertification expansion dominated by climate change were mainly distributed in the northeastern Hunshandake and the southeastern Mu Us sandy regions. The distribution of the desertification expansion regions mainly induced by human activity was relatively scattered and were mainly distributed in southwest Hunshandake, most of Chahar, western Hulunbeir and in the Mu Us and southeastern Horqin sandy regions. The regions that had experienced desertification expansion induced by both climate change and human activity were mainly found at the common boundary of the Hunshandake and Horqin sandy regions and in the middle of Bashang and Wulanchabu sandy regions.

4. Discussion

Desertification is a typical form of land degradation that is induced by climate change and human activity, and the differences between these driving forces mean that the desertified land and its dynamics have considerable spatial heterogeneity at the larger scale (Peters and Havstad, 2006; Prince, 2002; Yang et al., 2007). The farming-pastoral region of North China covers multiple climate zones and administrative regions from east to west, which makes the desertification driving factors, such as rainfall, temperature, population, land use and their trends vary greatly. The variations and differences among these driving factors made the farming-pastoral region of North China experience significant desertification dynamics between 2000 and 2010. Owing to the relative coarser resolution of MODIS images, great spatial heterogeneity of the research region and the modeling errors, it was difficult to get a perfect

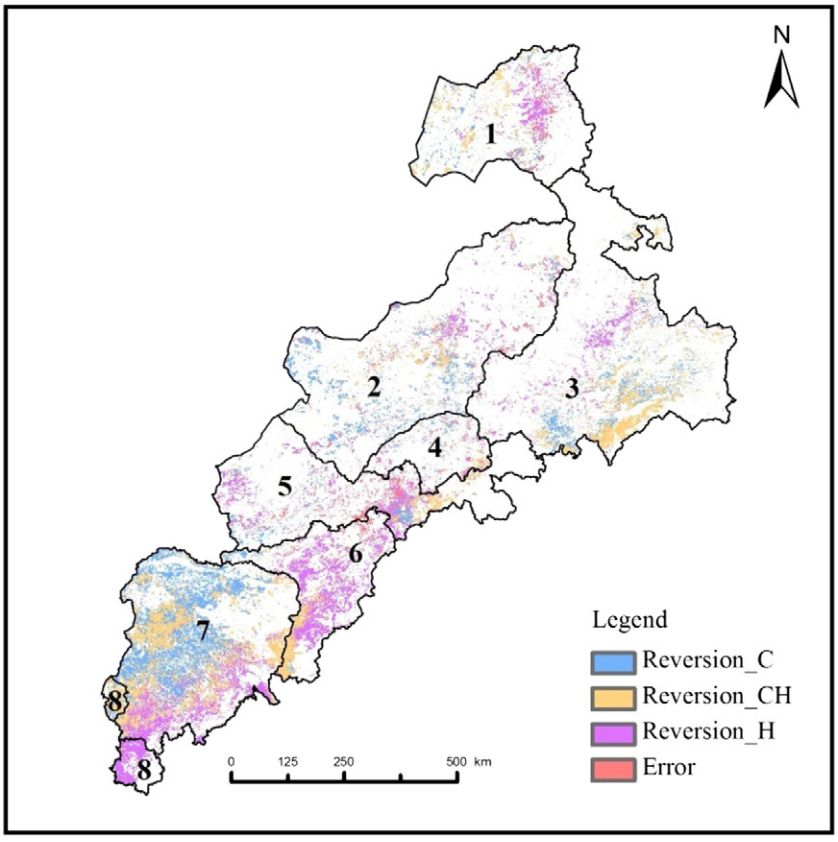

Fig. 5. The spatial distribution of lands had experienced desertification reversion of the farming-pastoral region of North China between 2000 and 2010 dominated by climate change and human activity.

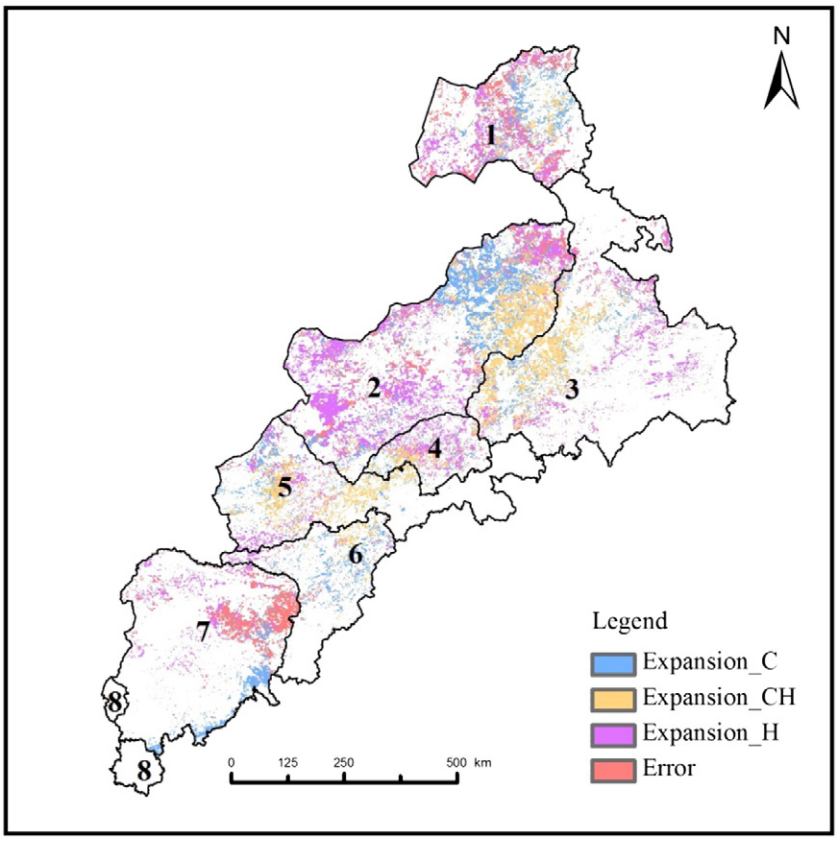

Fig. 6. The spatial distribution of lands had experienced desertification expansion of the farming-pastoral region of North China between 2000 and 2010 dominated by climate change and human activity.

monitoring accuracy. In order to improve the accuracy, special rules of DT model were constructed for each sub-region by considering the spatial heterogeneity. The monitoring results in this study generally reflected the actual desertification dynamics in the research region, which were consistent with the fourth desertification monitoring program in China launched by the State Forestry Administration and the research conducted by Wang et al. in 2011 (State Forestry Administration of China, 2011; Wang et al., 2011). All these monitoring results showed that the desertification reversion and expansion were actively occurring in the farming-pastoral region of North China between 2000 and 2010. Although the total area of desertified land in the research region had not changed significantly, an obvious desertification reversion in some regions in the farming-pastoral region of North China had been observed, such as the Mu Us sandy region.

Based on a uniform definition and assessment standard, desertification dynamics can be accurately monitored by using remote sensing images (Collado et al., 2002; Li et al., 2013; Yang et al., 2007); however, analyzing the relationship between desertification dynamics and their driving forces at the pixel scale is still a problem that needs to be solved (Geerken and Ilaiwi, 2004). In this study, the desertification dynamics in a fixed period were assumed to be the results induced by these two kinds of driving forces, and the relationship between desertification dynamics and climate change and human activity could be analyzed by comparing the trends in CNPP and HNPP for a target pixel. Similar to the previous research conducted at city level (Xu et al., 2009), this method is also proved to be suitable for investigating the relationship between desertification dynamics and their driving forces at regional scale in this study. However, the results derived using this method must be compared and explained at a specific scale, such as the dominated desertification driving processes at the sandy region scale and those at the whole research region scale were not completely the same in this study (Table 1). It was impossible to avoid errors when analyzing this relationship because completely accurate monitoring or classification cannot be achieved using remote sensing, especially at a coarse level (Huang and Siegert, 2006; Qi et al., 2012). Besides, the errors from NPP modeling would have an impact on the results, but the trend analysis at the pixel level used in this study would reduce these systematical errors. Owing to the large area of research region, the "error" regions identified in the assessment of relationship between desertification dynamics and driving forces was larger than previous studies at small scale (Xu et al., 2009). However, the proportion of these "error" regions to the total reversed and expanded desertification lands in this study was only 6.7% and 17.6% respectively, which would not affect the results for the whole research region.

Climate change is one of the most important factors affecting desertification dynamics (Nicholson et al., 1998; Prince et al., 1998; Sivakumar, 2007; Wang et al., 2005). Taking the research region as a whole, the aridity/humidity index (calculated as a proportion of evapotranspiration to rainfall) for the farming-pastoral region of North China between 2000 and 2010 showed a warm and humid trend, which indicated that the climate change would benefit the desertification reversion between 2000 and 2010. However, this trend analysis cannot totally explain the desertification dynamics in the research region because it ignores the spatial heterogeneity of climate change and desertification. In reality, the spatial heterogeneity of different climate factors means that climate change will have different effects on the regions that have experienced desertification reversion and expansion, and these differences can be captured and illustrated by using the method employed in this study. For example, the average trend of rainfall, temperature, average wind speed in spring and the aridity/humidity index in the regions that had experienced desertification reversion and expansion dominated by climate change were not the same (Fig. 7). These differences, together with the effects of other factors, such as soil and vegetation, made the changing trend of potential NPP vary greatly.

The average trend of climate factors confirmed the results of this study to some degree. For example, the regions that had experienced desertification reversion dominated by climate change always had a more humid land surface environment for vegetation rehabilitation than those regions that had experienced desertification expansion, and this could be mostly attributed to increased rainfall and a decrease in spring wind speed between 2000 and 2010. Although the average trends in climate factors were not able to differentiate spatial differences at a finer scale, they could reflect their relative contribution to the impact of climate change on desertification dynamics; and this might be further explored in the future studies by using the partial regression model or sensitivity analysis.

Human activity also had a significant impact on desertification dynamics in the farming-pastoral region of North China between 2000 and 2010. Since 2000, the Chinese government has launched many ecology protection projects and policies, such as the Beijing and Tianjin Sand Source Control Project, the Three-North Shelterbelt Project (phase III), Returning Farmland to Forest and Grassland and a policy of enclosed and grazing forbidden (Qi et al., 2012; Wang et al., 2007, 2011, 2013). These have made a great contribution to desertification reversion in the farming-pastoral region of North China between 2000 and 2010, which is partly reflected in the statistic data for cumulative afforestation area and sown pasture area since 2000 in the Inner Mongolian Autonomous Region, one of the biggest provinces in the farming-pastoral region of North China (Fig. 8). Nevertheless, there are considerable differences in the management and implementation of these projects and policies among different administrative regions, which is becoming an unstable factor for vegetation rehabilitation and desertification reversion. Excessive land use behaviors in some regions have not been completely stopped, which combined with rapid urbanization, the development of animal husbandry and the over-exploitation of mineral resources, making many regions in the farming-pastoral region of North China experience human-induced desertification expansion between 2000 and 2010. For example, the number of sheep and goats and total energy production of the Inner Mongolian Autonomous Region increased quickly after 2000 (Fig. 8c and d). Similar to the RESTREND method, the regions that had experienced human-induced desertification reversion and expansion were identified by analyzing the trend of HNPP in this study, and it would be possible to show the relationship between desertification dynamics and human activity in space. However, the validation and accuracy assessment were very difficult and it needed support from field inventory data and remote sensing images at a finer level (Brinkmann et al., 2011; Geerken and Ilaiwi, 2004). In this study, two sites that had experienced human induced desertification were also identified by comparing the Landsat ETM + images acquired in 2000 and the Aster images acquired in 2010 using the significant characteristics of human activity, and these were then used to validate the results from this study (Figs. 9 and 10). According to the comparisons in Figs. 9 and 10, the human induced desertification reversion and expansion could be identified by using the method mentioned above. For example, in Fig. 9, the desertification reversion induced by the development of villages and vegetation construction (regions in yellow circles) by local people could clearly be identified by comparing the images in 2000 and 2010, and these were almost consistent with the results derived from this study. Fig. 10 shows the damage to the vegetation rehabilitation region that already existed in 2000 (regions in yellow circles) and this can be attributed to human activity, and these areas were also identified in this study.

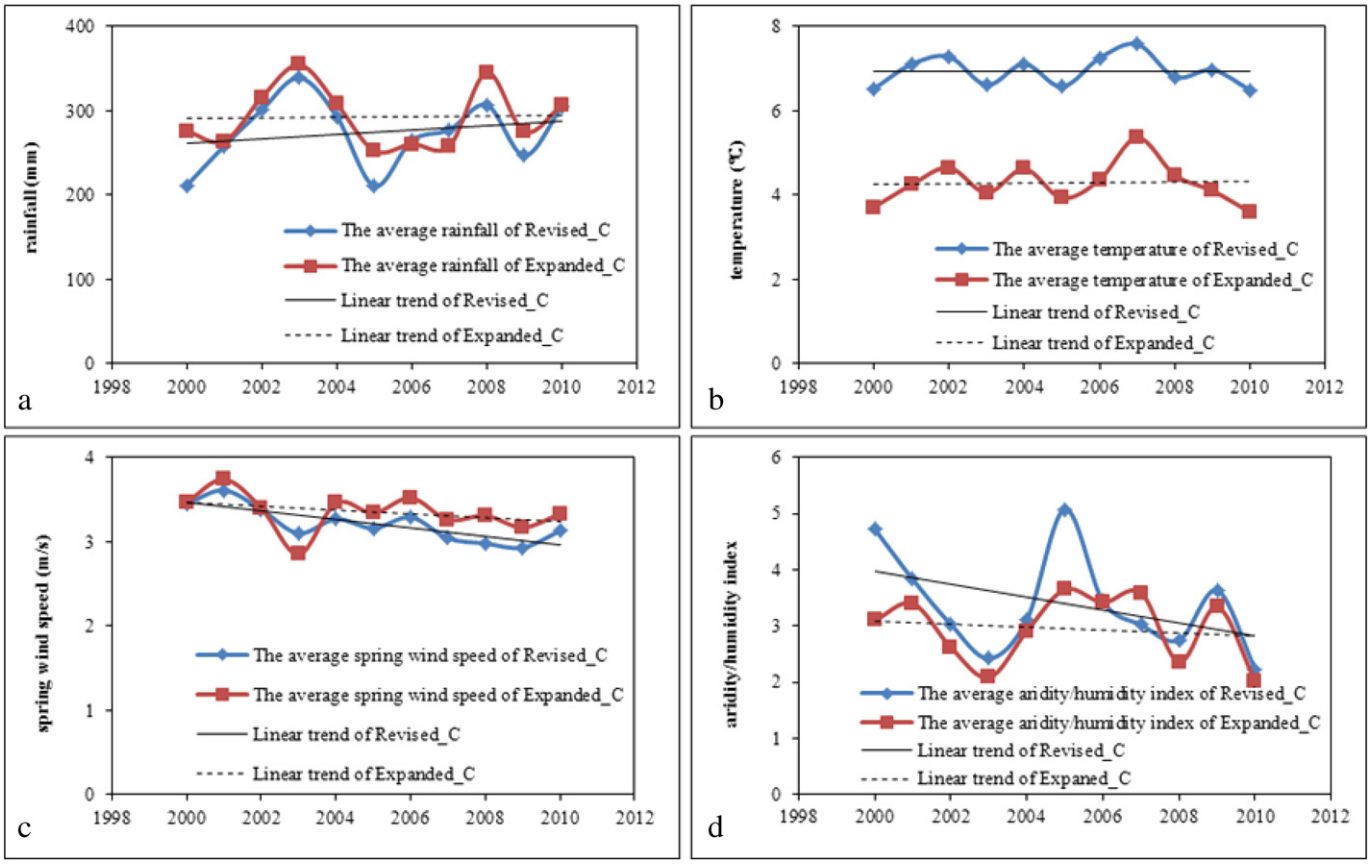

Fig. 7. The trends of some climate factors for the lands had experienced desertification reversion dominated by climate change between 2000 and 2010. (a) rainfall; (b) temperature; (c) spring wind speed; (d) aridity/humidity index.

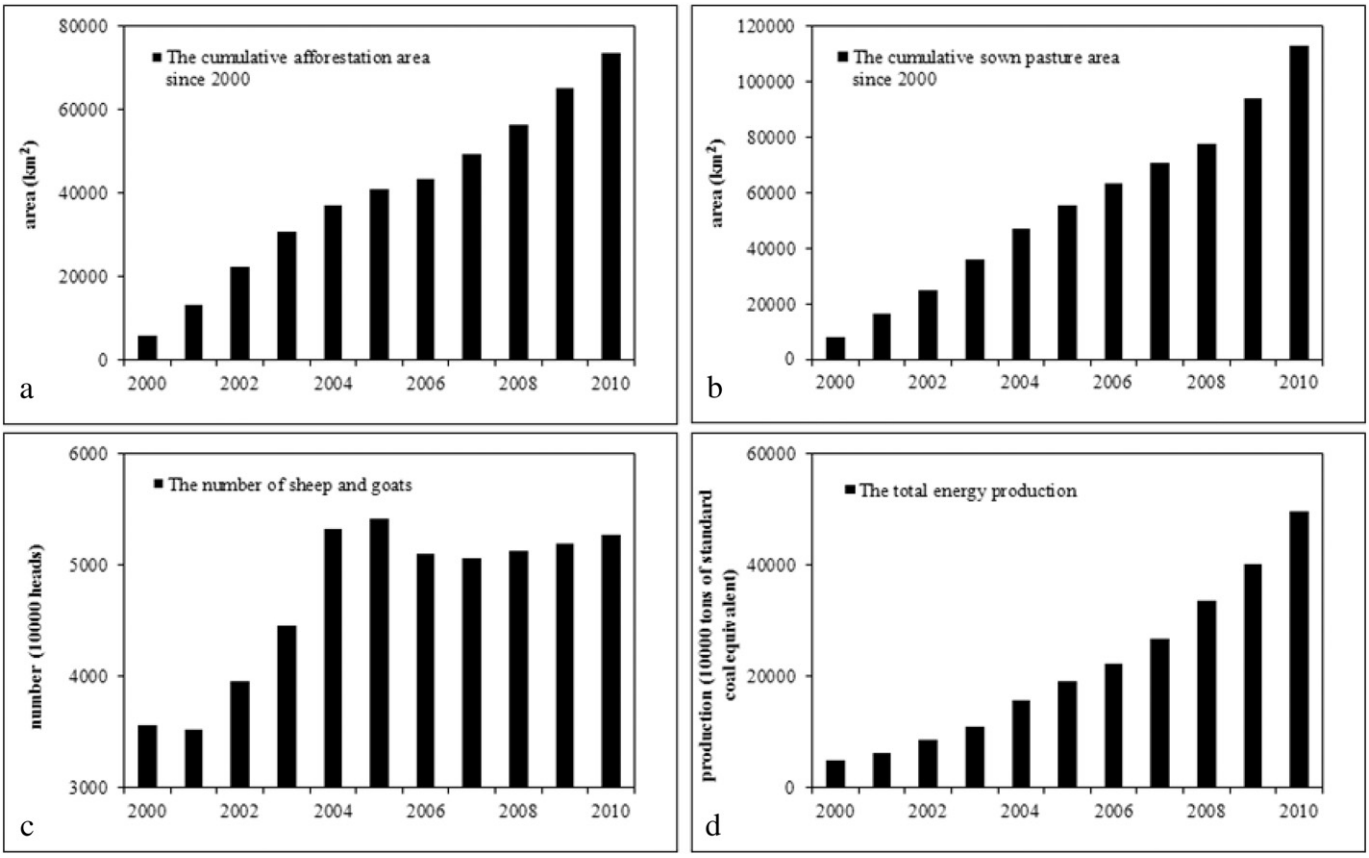

Fig. 8. The trends of some human activity indicators of Inner Mongolia between 2000 and 2010. (a) the cumulative afforestation area science 2000; (b) the cumulative sown pasture area science 2000; (c) the number of sheep and goats; (d) the total energy production.

5. Conclusions

The farming-pastoral region is an important desertified region in North China and monitoring the desertification dynamics and identifying their relationship with climate change and human activity in this region are fundamental for regional ecology and environment rehabilitation. The desertification monitoring results based on MODIS images showed that the farming-pastoral region had experienced significant desertification dynamics between 2000 and 2010, and the structure of the different desertification grades had changed considerably. The areas that had experienced desertification reversion and expansion were almost the same, but the spatial distribution of these regions was significantly different.

Climate change and human activity induced the desertification of the farming-pastoral region of North China between 2000 and 2010, but their relationship with desertification reversion and expansion were different and considerable spatial heterogeneity existed, and these were identified by analyzing and comparing the changing trends in potential NPP and the difference between potential and actual NPP for each pixel that had experienced desertification dynamics. The coupling of climate change and human activity was the relatively dominant factor affecting desertification reversion. However, human activity was the dominant factor that caused desertification expansion compared to other factors. The spatial heterogeneity of driving forces and their effects on desertification meant that the main driving processes in the sub-regions were significantly different. The results of this study can

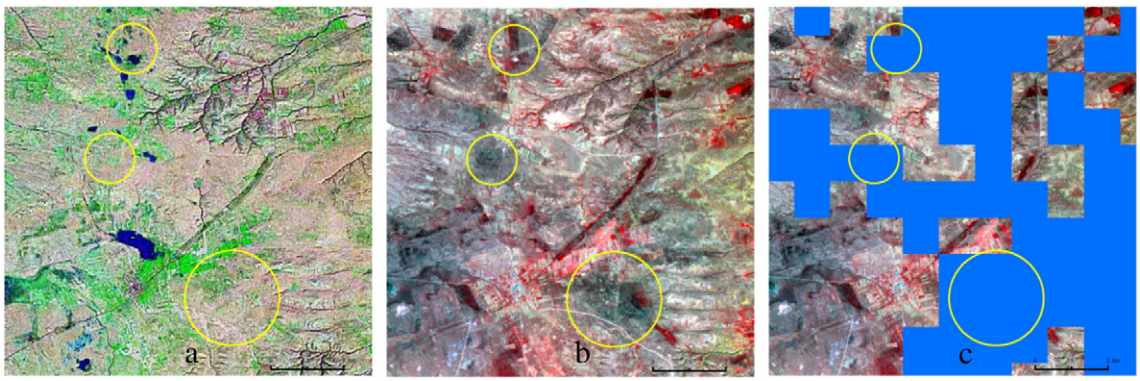

Fig. 9. The identification of human-induced desertification reversion and its validation by comparing ETM+ image in 2000 and Aster image in 2010. (a) ETM+ image in 2000; (b) Aster image in 2010; (c) the areas (blue regions) had experienced human-induced desertification reversion identified in this study.

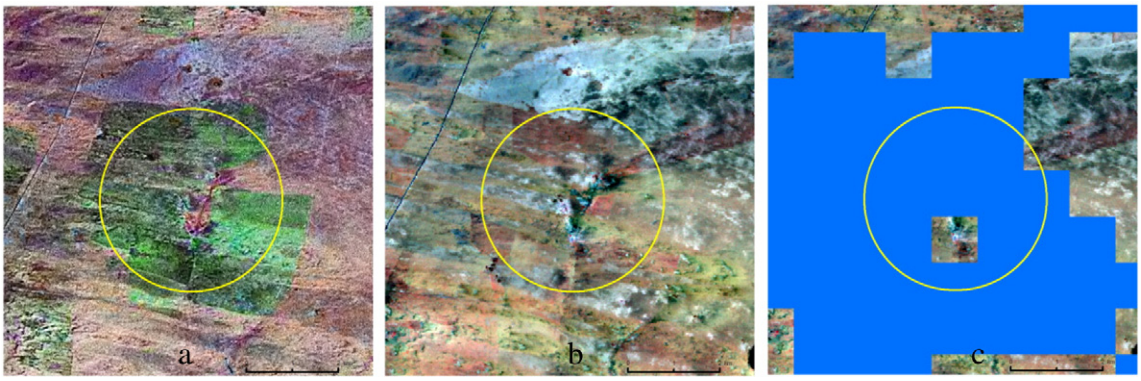

Fig. 10. The identification of human-induced desertification expansion and its validation by comparing ETM + image in 2000 and Aster image in 2010. (a) ETM + image in 2000; (b) Aster image in 2010; (c) the areas (blue regions) had experienced human-induced desertification expansion identified in this study.

be used to assess the effects of the implementation of ecological protection projects and policies. Although the details of the driving factors behind climate change and human activity had been discussed in this study, their relative roles in desertification dynamics need to be further investigated by using more data and other quantitative models.

Acknowledgments

This research is jointly supported by the National Key Technologies R&D Program of China (2012BAC19B09), and the Project 71103170 and the Project 40901054 supported by the National Natural Science Foundation of China. The authors also wish to thank the reviewers for their comments and suggestions.

References

Asner, G.P., Heidebrecht, K.B., 2005. Desertification alters regional ecosystem–climate interactions. Glob. Chang. Biol. 11, 182–194.
Brinkmann, K., Dickhoefer, U., Schlecht, E., Buerkert, A., 2011. Quantification of aboveground rangeland productivity and anthropogenic degradation on the Arabian Peninsula using Landsat imagery and field inventory data. Remote Sens. Environ. 115, 465–474.
Chen, Y.H., Li, X.B., Su, W., Li, Y., 2008. Simulating the optimal land-use pattern in the farming-pastoral transition zone of Northern China. Comput. Environ. Urban. Syst. 32, 407–414.
Collado, A.D., Chuvieco, E., Camarasa, A., 2002. Satellite remote sensing analysis to monitor desertification process in the crop–rangeland boundary of Argentina. J. Arid Environ. 52, 121–133.
Del Barrio, G., Puigdefabregas, J., Sanjuan, M.E., Stellmes, M., Ruiz, A., 2010. Assessment and monitoring of land condition in the Iberian Peninsula, 1989–2010. Remote Sens. Environ. 114, 1817–1832.
Evans, J., Geerken, R., 2004. Discrimination between climate and human-induced dryland degradation. J. Arid Environ. 57, 535–554.
Field, C.B., Randerson, J.T., Malmstrom, C.M., 1995. Global net primary production: combining ecology and remote sensing. Remote Sens. Environ. 51, 74–88.
Geerken, R., Ilaiwi, M., 2004. Assessment of rangeland degradation and development of a strategy for rehabilitation. Remote Sens. Environ. 90, 490–504.
Hanafi, A., Jauffret, S., 2008. Are long-term vegetation dynamics useful in monitoring and assessing desertification processes in the arid steppe, southern Tunisia. J. Arid Environ. 72, 557–572.
Hao, H.M., Ren, Z.Y., 2009. Land use/land cover change (LUCC) and eco-environment response to LUCC in farming-pastoral zone, China. Agric. Sci. China 8, 91–97.
Hein, L., de Ridder, N., 2006. Desertification in the Sahel: a reinterpretation. Glob. Chang. Biol. 12, 751–758.
Herrmann, S.M., Anyamba, A., Tucker, C.J., 2005. Recent trends in vegetation dynamics in the African Sahel and their relationship to climate. Glob. Environ. Change 15, 394–404.
Hill, J., Dach, C., Del Barrio, G., Stellmes, M., Hellden, U., Wang, C.Y., 2010. Integrating MODIS-EVI and gridded rainfall/temperature fields for assessing land degradation dynamics in Horqin sandy lands, Inner Mongolia (China). 30th EARSeL Symposium: Remote Sensing for Science, Education and Culture, 31 May–3 June 2010, UNESCO, Paris, France. Rainer Reuter, pp. 247–254.
Holm, A.M., Cridland, S.W., Roderick, M.L., 2003. The use of time-integrated NOAA NDVI data and rainfall to assess landscape degradation in the arid shrubland of Western Australia. Remote Sens. Environ. 85, 145–158.
Huang, S., Siegert, F., 2006. Land cover classification optimized to detect areas at risk of desertification in North China based on SPOT Vegetation imagery. J. Arid Environ. 67, 308–327.
Ji, L., Zhang, L., Wylie, B., 2009. Analysis of dynamic thresholds for the normalized difference water index. Photogramm. Eng. Remote. Sens. 75, 1131–1139.
Jiang, W.G., Li, J., Li, J.H., Chen, Y.H., Wu, Y.F., 2005. Changes and spatial patterns of eco-environment in the farming-pastoral region of northern China. J. Geogr. Sci. 15, 329–336.
Li, J.Y., Yang, X.C., Jin, Y.X., Huang, W.G., Zhao, L.N., Gao, T., Yu, H.D., Ma, H.L., Qin, Z.H., Xu, B., 2013. Monitoring and analysis of grassland desertification dynamics using Landsat images in Ningxia, China. Remote Sens. Environ. 138, 19–26.
Liu, J.H., Gao, J.X., Lv, S.H., Han, Y.W., Nie, Y.H., 2011. Shifting farming-pastoral ecotone in China under climate and land use changes. J. Arid Environ. 75, 298–308.
Lobell, D.B., Asner, G.P., Ortiz-Monasterio, J.I., Benning, T.L., 2003. Remote sensing of regional crop production in the YaquiValley, Mexico: estimates and uncertainties. Agric. Ecosyst. Environ. 94, 205–220.
Nicholson, S.E., Tucker, C.J., Ba, M.B., 1998. Desertification, drought, and surface vegetation: an example from the West African Sahel. Bull. Am. Meteorol. Soc. 79, 815–829.
Peters, D.P.C., Havstad, K.M., 2006. Nonlinear dynamics in arid and semi-arid systems: interactions among drivers and processes across scales. J. Arid Environ. 65, 196–206.
Potter, C.S., Randerson, J.T., Field, C.B., Matson, P.A., Vitousek, P.M.V., Mooney, H.A., Steven, A.K., 1993. Terrestrial ecosystem production: a process model based on global satellite and surface data. Glob. Biogeochem. Cycles 7, 811–841.
Prince, S.D., 2002. Spatial and temporal scales for detection of desertification. In: Reynolds, J.F., Stafford Smith, D.M. (Eds.), Global Desertification: Do Humans Cause Deserts? Dahlem University Press, Berlin (2).
Prince, S.D., De Colstoun, E.B., Kravitz, L.L., 1998. Evidence from rain-use efficiencies does not indicate extensive Sahelian desertification. Glob. Chang. Biol. 4, 359–374.
Prince, S.D., Wessels, K.J., Tucker, C.J., Nicholson, S.E., 2007. Desertification in the Sahel: a reinterpretation of a reinterpretation. Glob. Chang. Biol. 13, 1308–1313.
Prince, S.D., Becker-Reshef, I., Rishmawi, K., 2009. Detection and mapping of long-term land degradation using local net production scaling: application to Zimbabwe. Remote Sens. Environ. 113, 1046–1057.
Qi, Y.B., Chang, Q.R., Jia, K.L., Liu, M.Y., Liu, J., Chen, T., 2012. Temporal–spatial variability of desertification in an agro-pastoral transitional zone of northern Shaanxi Province, China. Catena 88, 37–45.
Sivakumar, M.V.K., 2007. Interactions between climate and desertification. Agric. For. Meteorol. 142, 143–155.
State Forestry Administration of China, 2011. The 4th Public Report of the Desertification and Sandy Desertification in China.
Su, Y.Z., Zhao, W.Z., Su, P.X., Zhang, Z.H., Wang, T., Ram, R., 2007. Ecological effects of desertification control and desertified land reclamation in an oasis-desert ecotone in an arid region: a case study in Hexi Corridor, northwest China. Ecol. Eng. 29, 117–124.
Tang, H.P., Zhang, X.S., 2003. Establishment of optimized eco-productive paradigm in the farming-pastoral zone of North China. Acta Bot. Sin. 45, 1166–1173.
Tao, F.L., Yokozawa, M., Zhang, Z., Xu, Yinlong, Hayashi, Y., 2005. Remote sensing of crop production in China by production efficiency models: models comparisons, estimate and uncertainties. Ecol. Model. 183, 385–396.
Veron, S.R., Paruelo, J.M., Oesterheld, M., 2006. Assessing desertification. J. Arid Environ. 66, 751–763.
Wang, T., 2004. Study on sandy desertification in China-3. Key regions for studying and combating sandy desertification. J. Desert Res. 24, 1–9 (in Chinese).
Wang, T., Wu, W., Chen, G.T., Xue, X., Sun, Q.W., 2004a. Study of spatial distribution of sandy desertification in North China in recent 10 years. Sci. China Ser. D Earth Sci. 47 (z1), 78–88.
Wang, T., Wu, W., Xue, X., Sun, Q.W., Zhang, W.M., Han, Z.W., 2004b. Spatial–temporal changes of sandy desertified land during last 5 decades in northern China. Acta Geograph. Sin. 59, 203–212 (in Chinese).
Wang, X.M., Chen, H.F., Hasi, E., 2005. Desertification in China: an assessment. Earth Sci. Rev. 88, 188–206.
Wang, X.H., Lu, C.H., Fang, J.F., Shen, Y.C., 2007. Implications for development of grain-for-green policy based on cropland suitability evaluation in desertification-affected North China. Land Use Policy 24, 417–424.
Wang, T., Song, X., Yan, C.Z., Li, S., Xie, J.L., 2011. Remote sensing analysis on aeolian desertification trends in northern China during 1975–2010. J. Desert Res. 31, 1351–1356 (in Chinese).

Wang, F., Pan, X.B., Wang, D.F., Shen, C.Y., Lu, Q., 2013. Combating desertification in China: past, present and future. Land Use Policy 31, 311–313.
Wessels, K.J., Prince, S.D., Frost, P.E., VanZyl, D., 2004. Assessing the effects of human-induced land degradation in the former homelands of northern South Africa with a 1 km AVHRR NDVI time-series. Remote Sens. Environ. 91, 47–67.
Wessels, K.J., Prince, S.D., Malherbe, J., Small, J., Frost, P.E., VanZyl, D., 2007. Can human-induced land degradation be distinguished from the effects of rainfall variability? Acase study in South Africa. J. Arid Environ. 68, 271–297.
Wessels, K.J., Prince, S.D., Reshef, I., 2008. Mapping land degradation by comparison of vegetation production to spatial derived estimates of potential production. J. Arid Environ. 72, 1940–1949.
Xu, D.Y., Kang, X.W., Liu, Z.L., Zhuang, D.F., Pan, J.J., 2009. Assessing the relative role of climate change and human activity in sandy desertification of Ordos region, China. Sci. China Ser. D Earth Sci. 56, 855–868.
Xu, D.Y., Kang, X.W., Zhuang, D.F., Pan, J.J., 2010. Multi-scale quantitative assessment of the relative roles of climate change and human activity in desertification—a case study of the Ordos Plateau, China. J. Arid Environ. 74, 498–507.
Yang, X., Ding, Z., Fan, X., Zhou, Z., Ma, N., 2007. Processes and mechanisms of desertification in northern China during the last 30 years, with a special reference to the Hunshandake Sandy land, eastern Inner Mongolia. Catena 71, 2–12.
Zarco-Tejada, P.J., Rueda, C.A., Ustin, S.L., 2003. Water content estimation in vegetation with MODIS reflectance data and model inversion methods. Remote Sens. Environ. 85, 109–124.